Journal of Data Acquisition and Processing
ISSN: 1004-9037
https://sjcjycl.cn/
DOI: 10.5281/zenodo.7778386

PERFORMANCE EVALUATION OF A NOVEL SVPWM CONTROL STRATEGY FOR RECTIFIERS CONNECTED TO VEHICLE ENERGY STORAGE SYSTEMS

S.Md.Mazhar-ul –haq
Research Scholar, Dept of EEE, JNTU Hyderabad

Dr.S.S.Tulasi Ram
Professor, Dept. of EEE, JNTUH College of Engineering, Hyderabad

Dr. J.B.V .Subrahmanyam
Professor, Dept. of EEE, Siddhartha Institute of Technology and Sciences, Hyderabad

***Abstract*—**This research describes a three-phase rectifier that can process three different DC voltages (low, medium, and high) at once. In this research, we assess and analyze a modified double-loop decoupling SVPWM approach based on asymmetric two-level vector space for transferring energy directly from the AC port to the low voltage DC port inside single-stage power conversion. The low voltage port with the broad voltage range may get power straight from the AC grid thanks to the rectifier and the improved SVPWM management technique. As a result, we may use a lower-rated downstream DC-DC converter and fewer stages of power conversion. Compared to the conventional two-stage rectifier, which consists of a three-phase two-level rectifier wired to the vehicle's energy storage system, the given architecture and vector space are distinctive. Matlab-Simulink was used to model the system and show that lower harmonics lead to greater performance.

Keywords-Double-loop decoupling SVPWM; current controller; harmonics mitigation; power quality;

I. Introduction

The primary function of three-phase rectifiers is to connect high-power DC loads to an alternating current (AC) power supply. High power factor of line current, high efficiency, simple modulation pattern, and control diagram 0 make boost type rectifiers the most popular form of three phase rectifier. Other common types are buck type and buck-boost type rectifiers. The boost type rectifier's output voltage, however, must be higher than the maximum value of the AC line voltage. Over modulation and distortion of grid-side current will occur if the DC output voltage is less than the peak value of the line voltage, even when using an SVPWM technique. To connect the high DC voltage to the vehicle battery, as seen in Fig. 1, a down-stream voltage step-down DC-DC converter is required. Thus, all energy must undergo double processing, lowering conversion efficiency. When the output voltage of a boost type rectifier is less than the maximum value of the AC line voltage, the rectifier will not function correctly. However, the foregoing problems can be avoided by using customised SVPWM rectifiers. They are more efficient, have a higher power factor, and a bidirectional power flow, while also lowering the higher harmonics and improving the sinusoidal current on the grid side. As a result, it has greater support in the academic community and finds widespread use in high-

performance power electronics. In this research, we use MATLAB/Simulink to investigate a double-loop decoupled SVPWM rectifier and calculate the switch loss on a three-phase rectifier by employing various control strategies.

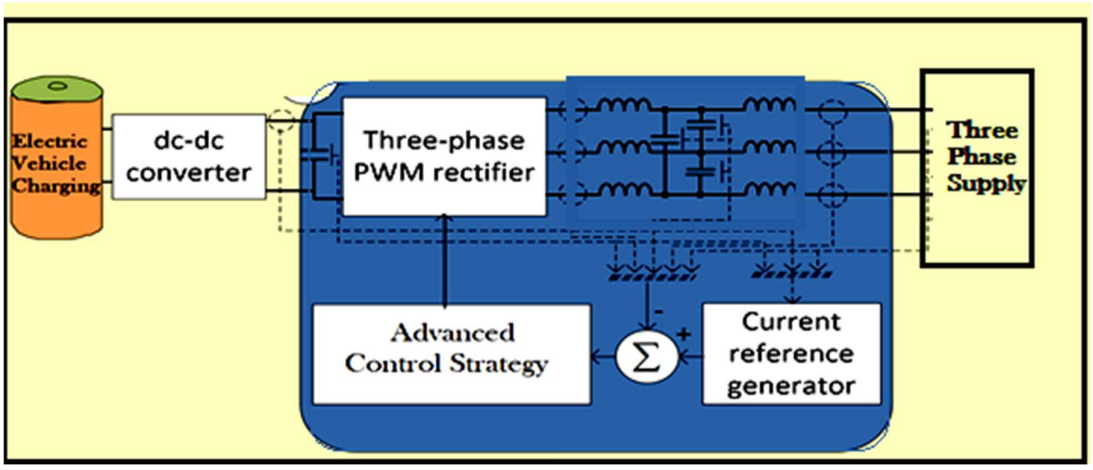

Figure 1 Block Diagram of considered work

The mathematical model of a three-phase rectifier and its associated control mechanism are examined as part of the PWM rectifier examination. At first, we examine the various rectifier topologies and their implications. The mathematical models of a three-phase PWM rectifier are next explored in detail. There are two main categories of mathematical models. Both are based on duty ratios and switches, but the former is more common. In addition, a d-p coordinate system analysis of a mathematical model of a three-phase rectifier is presented. The use of double-loop decoupled SVPWM control, as well as other techniques of controlling three-phase rectifiers, is discussed. The idea and implementation of SVPWM modulation are then described in depth. Three-phase rectifier control technique simulations are developed in MATLAB/Simulink. Dynamic responses of the approach are demonstrated. The simulation switch model is shown.

II. A mathematical model of a pulse width modulated (PWM) rectifier for a three-phase voltage source

By "generic mathematical model of a voltage source rectifier," researchers mean a mathematical description of a voltage source rectifier in three-phase static coordinate system phases (a, b, c) according to its topology using Kirchhoff's current law and Kirchhoff's voltage law as foundational principles. Figure 2 depicts the structure of a voltage source rectifier with three distinct phases and their respective labels.

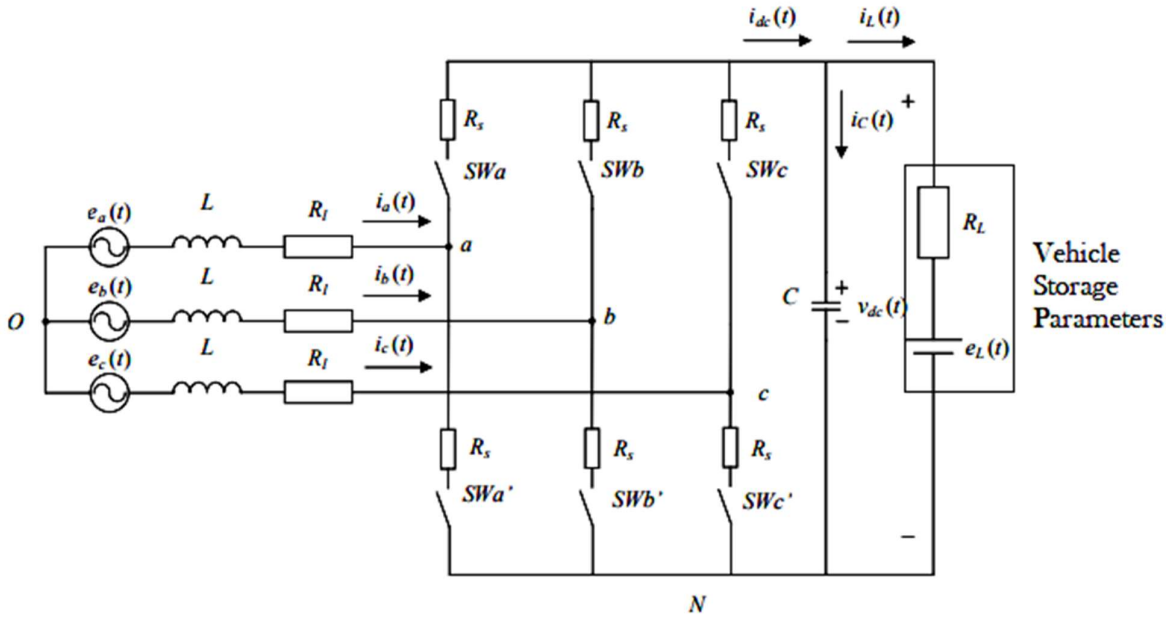

Figure 2 Mathematical Model of VSC

The standard mathematical model of a three-phase voltage source rectifier is constrained by the following assumptions:

1. The three-phase RMS values of an ideal sinusoidal symmetric electromotive force source (e_a, e_b, e_c).
2. An unsaturated linear grid-side inductor filter.
3. Thirdly, for each phase, R s is the equivalent resistance to the power loss caused by the power switches. In other words, we assume the power switch is a perfect series device with a loss resistance of R_s.The Vehicle load, which is a resistance R_L connected in series with an ideal Battery, simulates the three-phase voltage source rectifier's bidirectional power transfer (Vehicle Battery).

Similar to Figure 2, when Vehicle battery eL (t) = 0, the DC side load is entirely resistive. Here, the three-phase VSR can only function in rectification mode. Three-phase VSR can switch between rectification and active inverter modes depending on when eL (t) > vdc (t). While in active inverter mode, also known as regenerative power production mode, a three-phase VSR will send the DC-side power on eL (t) to the grid. The three-phase VSR can only function in rectification mode when eL (t) < vdc (t).

We define the boolean switch function sk of the three-phase rectifier power switch in the following way for ease of analysis:

$$s_k = \begin{cases} 1; \text{ The upper arm It's like someone flipped a switch: "Upper arm on, lower arm off."} \\ 0; \text{ The upper arm It's like someone flipped a switch: "Upper arm off, lower arm on."} \end{cases}$$

Where $k \in \{a, b, c\}$.

In this work, we combine the loss resistance R s of a three-phase VSR power switch with its corresponding loss resistance R_l as R, so $R = R_s + R_l$. Phase an of the three-phase VSR circuit formula is constructed by using Kirchhoff's voltage law (KVL) as follows:

$$L\frac{di_a}{dt} + Ri_a = e_a - (v_{aN} + v_{NO}) \ldots\ldots (1)$$

where $v_{NO} = v_N - v_O$ the voltage between point N and point O in Figure 2. When SWa is turned on and SWa′ is turned off, $s_a = 1$ and $v_{aN} = v_{dc}$. When SWa is turned off and SWa′ is turned on, $s_a = 0$ and $v_{aV} = 0$. Since $v_{aN} = v_{dc}s_a$, equation can be modified to:

$$L\frac{di_a}{dt} + Ri_a = e_a - (v_{dd}s_a + v_{NO}) \ldots (2)$$

Similarly for phases b and c:

$$L\frac{di_b}{dt} + Ri_b = e_b - (v_d s_b + v_{NO}) \ldots\ldots (3)$$

specified a three-phase symmetric scheme, we encompass

$$e_a + e_b + e_c = 0;\ i_a + i_b + i_c = 0 \ldots\ldots\ldots (4)$$

combine equations above three ,so

$$v_{NO} = -\frac{v_{dc}}{3}\sum_{k\in\{a,b,c\}} s_k \ldots\ldots (5)$$

In Figure 2, As a rule, just one of the bridge's arms will have its electricity on.so there are $2^3 = 8$ switching combinations in total. Hence, we can describe i_{dc} on the DC side as:

$$\begin{aligned} i_{dc} = {} & i_a s_a \bar{s}_b \bar{s}_c + i_b s_b \bar{s}_c \bar{s}_a + i_c s_c \bar{s}_b \bar{s}_a + (i_a + i_b) s_a s_b \bar{s}_c \\ & + (i_a + i_c) s_a s_c \bar{s}_b + (i_b + i_c) s_b s_c \bar{s}_a + (i_a + i_b + i_c) s_a s_b s_c \ldots (6) \\ = {} & i_a s_a + i_b s_b + i_c s_c \end{aligned}$$

The following is the whole switching function of the modelled VSC block diagram implementation:

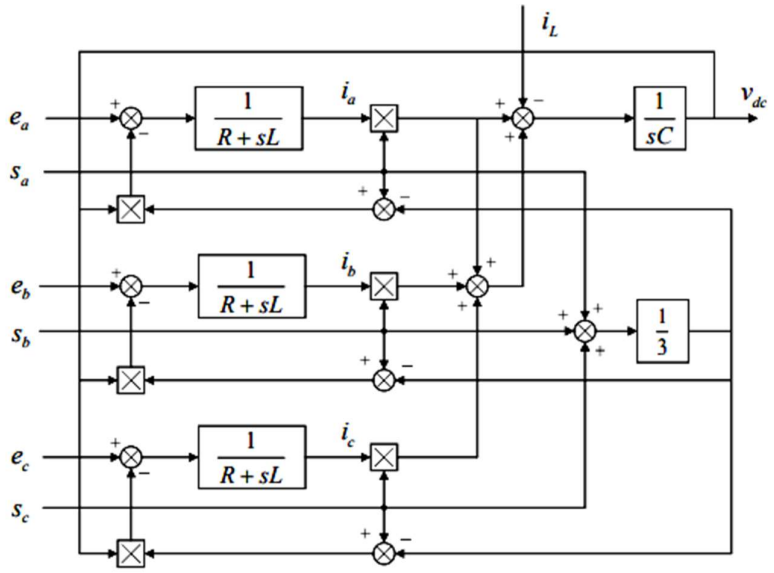

Figure 3 switching function mathematical model of Three phase VSC

III. Decoupled SVPWM control with two loops

After obtaining vd* and vq*, we no longer send them into the PWM Signal Generator, which is the primary difference between Double-loop decoupling SVPWM control and Double-loop decoupling SPWM control. Instead, we send the signals to a Space Vector Pulse Width Modulation (PWM) Signal Generator. The period of the triangle carrier wave is shown here by the symbol "Ts." Its basic outline may be seen in Figure 4.

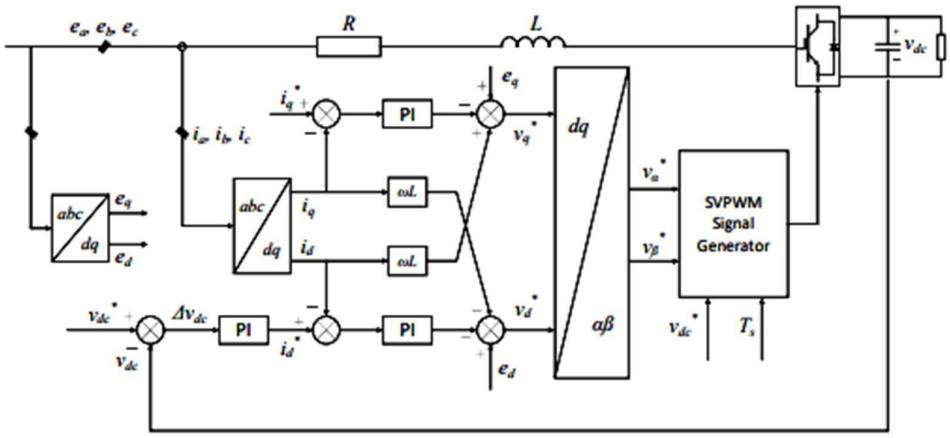

Figure 4 Double loop Decoupled SVPWM

There are eight possible permutations while switching, as noted before. Table 1 displays the phase-to-ground voltage and phase-to-phase voltage for each possible switching configuration.
Table 1: Phase-to-ground and phase-to-phase voltages for various switching arrangements

s_a	s_b	s_c	v_a	v_b	v_c	v_{ab}	v_{bc}	v_{ca}
0	0	0	0	0	0	0	0	0

1	0	0	$2v_{dc}/3$	$-v_{dc}/3$	$-v_{dc}/3$	v_{dc}	0	$-v_{dc}$
0	1	0	$-v_{dc}/3$	$2v_{dc}/3$	$-v_{dc}/3$	$-v_{dc}$	v_{dc}	0
1	1	0	$v_{dc}/3$	$v_{dc}/3$	$-2v_{dc}/3$	0	v_{dc}	$-v_{dc}$
0	0	1	$-v_{dc}/3$	$-v_{dc}/3$	$2v_{dd}/3$	0	$-v_{dc}$	v_{dc}
1	0	1	$v_{dc}/3$	$-2v_{dd}/3$	$v_{dc}/3$	v_{dc}	$-v_{dc}$	0
1	1	0	$v_{dc}/3$	$v_{dc}/3$	$-2v_{dc}/3$	$-v_{dc}$	0	v_{dc}
1	1	1	0	0	0	0	0	0

All eight possible permutations may be conveniently represented on a complex plane by mapping them to vectors of norm $2v_{dc}/3$. In a plane, the six vectors (v_0 through v_{300}) create six equally sized sectors, with v_{000} and v_{111} being referred to as zero vectors due to their norm being zero. Phase voltages are obtained by projecting the space vector corresponding to each possible switching configuration onto the (a, b, c) coordinate system.

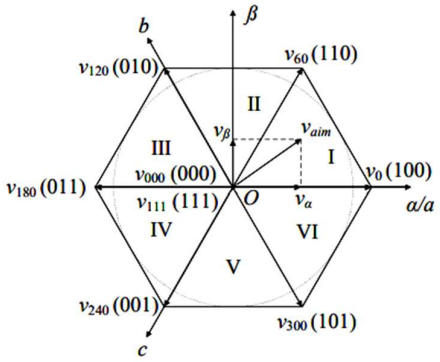

Figure 5 Statistical Analysis of Voltage Vectors

The current definition of v_{ref}, the reference vector in voltage space, is as follows:

$$v_{\text{ref}} = \frac{2}{3}\left(v_a + v_b e^{j2\pi/3} + v_c e^{j4\pi/3}\right) = v_\alpha + jv_\beta \ldots\ldots (7)$$

When v "ref" is projected to the (a,b,c) coordinate system, the norms of the corresponding phase voltages are v_a, v_b, v_c, and when v "ref" is projected to the(α, β)coordinate system, the norms of the corresponding phase voltages are v_α, v_β . Figure 5 shows that the terminus of the rotating vector v ref follows a quasi-circular path, rotating counterclockwise at a speed of ω.

Any of the six sectors' v "ref " may be constructed from the neighbouring vectors using the voltage-second balance.

SVPWM Modulation Realization

The switching time of the neighbouring vectors may be determined after first locating the reference vector, from which we learn the norm and phase angle of the vector, which in turn allows us to determine the time of switch-on using some logic. Only four of the six possible space vectors are nonzero; v_{000} and v_{111} are the zero vectors. The zero vectors' operational time is the time remaining in a switching period after all other vectors have been taken into account. For optimal performance, it is best to arrange the vectors, including the zero vectors, in such a way that switching events occur seldom. Moreover, we often choose a symmetric order for the operation of the vectors to achieve a symmetric PWM signal, which helps to reduce the impact of the signal's higher harmonics.

Before implementing SVPWM, a transformation from the three-phase static coordinate system to the two-phase static coordinate system is required to adjust the reference vector. The equation to represent the transition is:

$$\begin{bmatrix} v_\alpha \\ v_\beta \end{bmatrix} = \frac{2}{3}\begin{bmatrix} 1 & -\frac{1}{2} & -\frac{1}{2} \\ 0 & \frac{\sqrt{3}}{2} & -\frac{\sqrt{3}}{2} \end{bmatrix}\begin{bmatrix} v_a \\ v_b \\ v_c \end{bmatrix} \ldots\ldots (8)$$

1 **Nailing down the sector:**

According to Figure 5, when v_{ref} is in sector I, we get:

$$0 < arctan\left(\frac{v_\beta}{v_\alpha}\right) < \frac{\pi}{3} \ldots\ldots\ldots\ldots (9)$$

In adding up to the dissimilarity above taking into consideration the arithmetical relationship in Figure 5, we can bring to a close that the essential and sufficient circumstance of v_{ref} in sector I is:

$$v_\alpha > 0, v_\beta > 0 \text{ and } \frac{v_\beta}{v_\alpha} < \sqrt{3} \ldots\ldots (10)$$

Table 2 Essential and adequate circumstances of v_{ref} in Sector N

Sector	Necessary and Sufficient Condition
I	$v_\alpha > 0, v_\beta > 0$ and $\frac{v_\beta}{v_\alpha} < \sqrt{3}$
II	$v_\beta > 0$ and $\frac{v_\beta}{\lvert v_\alpha \rvert} > \sqrt{3}$
III	$v_\alpha < 0, v_\beta > 0$ and $-\frac{v_\beta}{v_\alpha} < \sqrt{3}$
IV	$v_\alpha < 0, v_\beta > 0$ and $\frac{v_\beta}{v_\alpha} < \sqrt{3}$

V	$v_\beta > 0$ and $-\frac{v_\beta}{\lvert v_\alpha \rvert} > \sqrt{3}$
VI	$v_\alpha > 0, v_\beta < 0$ and $-\frac{v_\beta}{v_\alpha} < \sqrt{3}$

The table above tells us that the vector may be found by determining whether or not the following expressions are bigger than zero.

$$\begin{cases} v_\beta, \\ \sqrt{3}v_\alpha - v_\beta, \ldots\ldots (11) \\ -\sqrt{3}v_\alpha - v_\beta \end{cases}$$

Here we describe variables A, B, C. When $v_\beta > 0, A = 1$, or else, $A = 0$. While $\sqrt{3}v_a - v_\beta > 0, B = 1$, or else, $B = 0$. While $-\sqrt{3}v_\alpha - v_\beta > 0, C = 1$, or else, $C = 0$. There are eight possible combinations of A, B, and C, with six of them having corresponding vectors whose norms are nonzero and the other two having norms of zero and corresponding to two separate sectors. N is defined as A+2B+4C for the sake of assessing the sectors more easily, and the resulting relationship between N and the associated sectors is shown in Table 3. Table 3. N and it corresponding sectors

Sector	I	II	III	IV	V	VI
N	3	1	5	4	6	2

2. Pinpointing the vector transitions

It was said previously in this chapter that the goal voltage vector may be obtained by composing it with two nearby vectors as base vectors and selecting an acceptable operation time of them to obtain the necessary proportion from the base vector. Figure 6 shows an example of a target voltage vector for sector I, and its associated switching function is shown in Figure 7. We insert a zero voltage vector v111 into the centre of the goal voltage vector with an operation time of T111, and we insert a zero voltage vector v000 into both the beginning and the end with an operation time of T000 / 2. In order to lessen the impact of PWM's higher harmonics, we symmetricize the switching function.

Following the following procedure, we get:

$$\begin{cases} t_{ona} = \dfrac{T_s - T_1 - T_2}{4} \\ t_{onb} = t_{on\,a} + \dfrac{T_1}{2} \ldots\ldots\ldots (12) \\ t_{onc} = t_{onb} + \dfrac{T_2}{2} \end{cases}$$

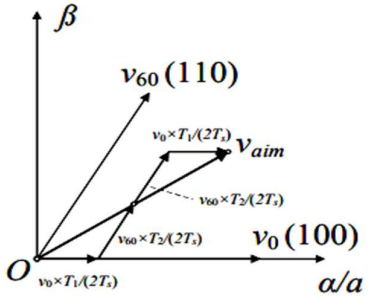

Figure 6 vector components

The switching time on additional sectors can be attained in a similar fashion, as in:

Table 4 Switching time in sectors

Switching Time	1	2	3	4	5	6
t_{onl}	$t_{\text{on b}}$	$t_{\text{on } a}$	$t_{\text{on } a}$	$t_{\text{on } c}$	$t_{\text{on } c}$	$t_{\text{on b}}$
$t_{\text{on 2}}$	$t_{\text{on } a}$	$t_{\text{on } c}$	$t_{\text{on } b}$	$t_{\text{on } b}$	$t_{\text{on } a}$	$t_{\text{on } c}$
$t_{\text{on 3}}$	$t_{\text{on } c}$	$t_{\text{on } b}$	t_{onc}	$t_{\text{on } a}$	$t_{\text{on } b}$	$t_{\text{on } a}$

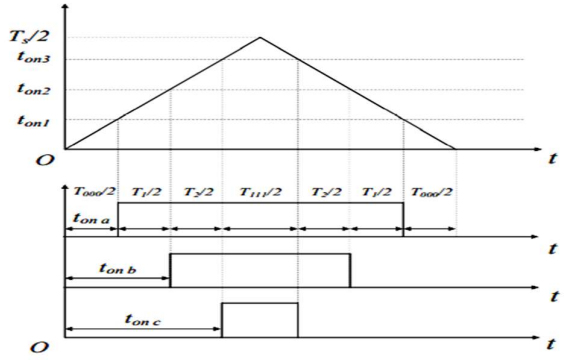

Figure 7 Vector I Switching Function Correspondent

IV. SIMULATION IMPLEMENTATION AND RESULTS

Parameters and Model of the System

A MATLAB/Simulink model is constructed to look like Figure 8. A three-phase balanced voltage supply is simulated by use of three regulated voltage sources. Three 50 Hz sine waves with 0°, 2/3*pi°, and 4/3*pi° phases are fed into them as input signals. The RMS value of the AC side phase voltage is 230 V and output was boosted to 700 V to charge the load. The input filter inductance on the AC side is 20 mH. The corresponding resistance on the AC side is only 0.2 ohms. R1 is a 200-ohm load on the DC side, while R2 is a 100-ohm load. The filter capacitor on the DC side has a value

of 680 F. The frequency of the carrier wave is 1104 Hz. The 3-phase half-bridge uses six MOSFETs.

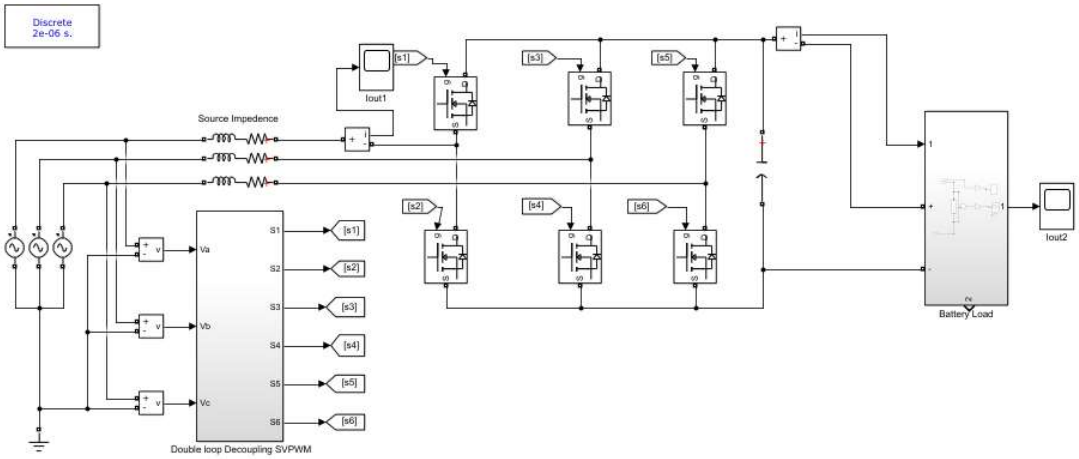

Figure 8 Simulink Implementation

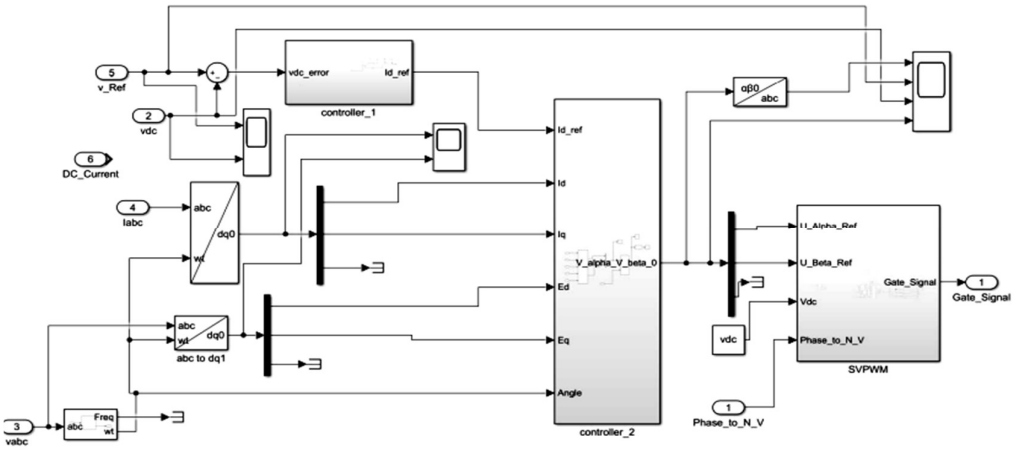

Figure 9 Control of Double Loop Decoupling SVPWM

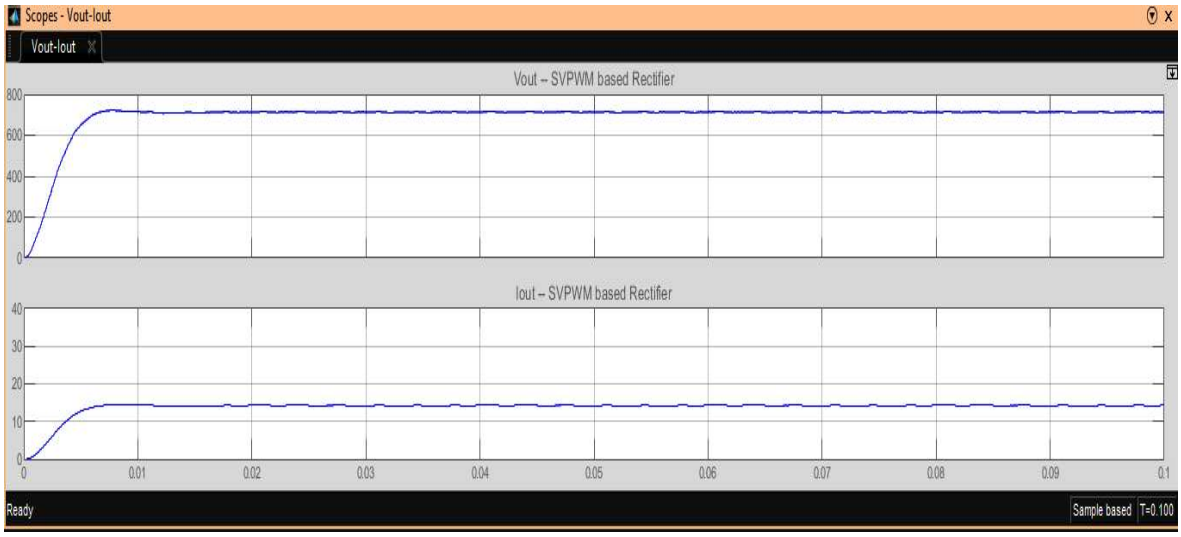

Figure 10 Output voltage and Current Waveforms

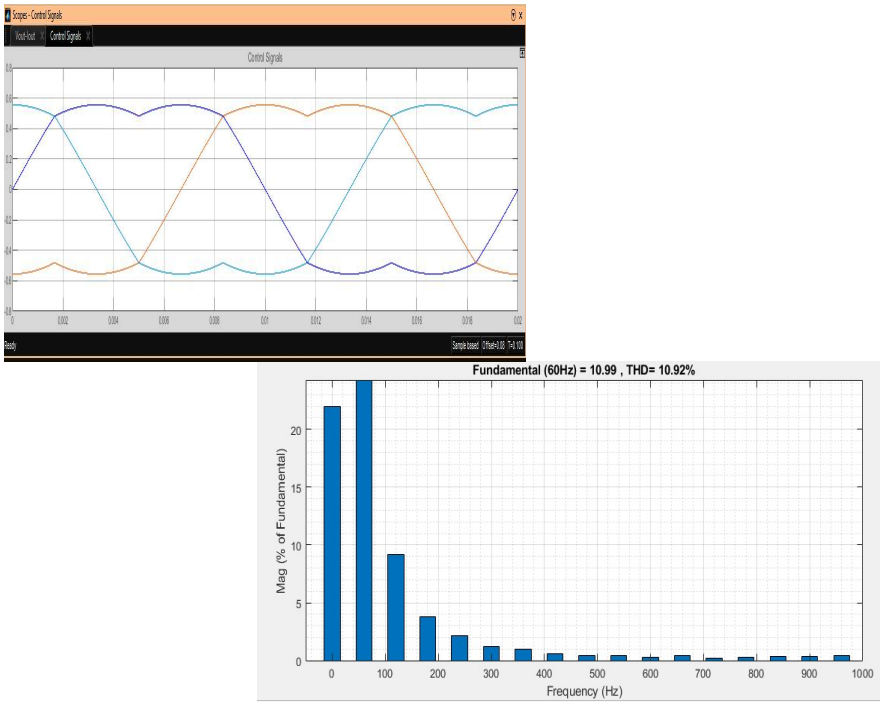

Figure 11 SVPWM output and THD

V. CONCLUSION

In this paper, we demonstrate and validate the use of a three-phase rectifier with a modified double decoupled SVPWM approach for high-efficiency and wide-voltage-range applications. Using boost type architecture, the described rectifier may move power straight from the AC grid to the low voltage. We conclude that the double-loop decoupling SVPWM method in three-phase VSR have the lowest power loss on switches and harmonic distortion when compared to conventional methods, respectively.

REFERENCES

[1] Y. Zou, L. Zhang, Y. Xing, Z. Zhang, H. Zhao and H. Ge, "Generalized Clarke Transformation and Enhanced Dual-Loop Control Scheme for Three-Phase PWM Converters Under the Unbalanced Utility Grid," in IEEE Transactions on Power Electronics, vol. 37, no. 8, pp. 8935-8947, Aug. 2022, doi: 10.1109/TPEL.2022.3153476

[2] S. Bayhan and H. Komurcugil, "Sliding-Mode Control Strategy for Three-Phase Three-Level T- Type Rectifiers With DC Capacitor Voltage Balancing," in IEEE Access, vol. 8, pp. 64555-64564, 2020, doi: 10.1109/ACCESS.2020.2980814

[3] Q. Jia, Y. Qi, X. Xiong, P. Ma, ―Research and Implementation of SWISS Rectifier Based on Fuzzy PI Control‖, 3rd International Conference on Mechanical, Control and Computer Engineering, 2018

[4] J. Ma, W. Song, S. Wang, X. Feng, ―Model Predictive Direct Power Control for Single Phase Three-Level Rectifier at Low Switching Frequency‖ IEEE Transactions on Power Electronics, Vol. 33, Iss.2, 2018

[5] H. Wu, J. Wang, T. Liu, T. Yang, Y. Xing, ―Modified SVPWM Controlled Three-Port Three-Phase AC-DC Converters with Reduced Power Conversion Stages for Wide Voltage Range Applications‖, IEEE Transactions on Power Electronics, Vol. 33 , Iss.8, 2018

[6] Y. Gui, M. Li, J. Lu, S. Golestan, J. M. Guerrero, and J. C. Vasquez, ―A Voltage Modulated DPC Approach for Three-Phase PWM Rectifier‖ IEEE Transactions on Industrial Electronics, Vol. 65 , Iss.10, 2018

[7] M. A. Rocha, W. G. de Souza, P. J. A. Serni, A.L. Andreoli, G. A. M. Clerice, P. S. da Silva, ―Control of Three-Phase PWM Boost Rectifiers Using Proportional-Resonant Controllers‖,SimposioBrasileiro de SistemasEletricos (SBSE), IEEE, 2018

[8] A. Fekik , H. Denoun , M. L. Hamida , A. T. Azar, M. Atig, Q. M. Zhu, ―Neural Network Based Switching State Selection For Direct Power Control of Three Phase PWM-Rectifier‖, 10th International Conference on Modelling, Identification and Control (ICMIC), IEEE, 2018

[9] X. Li, Y. Sun, H. Wang, M. Su, S. Huang, ―A Hybrid Control Scheme for Three-Phase Vienna Rectifiers‖, IEEE Transactions on Power Electronics, Vol. 33, Iss.1, 2018

[10] A. V. Nikitin, ―Holistic control of three-phase bidirectional rectifiers, IEEE National Aerospace and Electronics Conference, NAECON 2018

[11] D. Menzi, D. Bortis, J. W. Kolar, ―A New Bidirectional ThreePhase Phase-Modular Boost-Buck AC/DC Converter‖, IEEE International Power Electronics and Application Conference and Exposition (PEAC), 2018

[12] S. Xie , Y. Sun , M. Su , J. Lin , Q. Guang, ―Optimal switching sequence model predictive control for three-phase Vienna rectifiers‖, IET Electric Power Applications, Vol.12, Iss.7, 2018

[13] S. Hadjeras, C. A. Sanchez, F. Gomez-Estern Aguilar, F. Gordillo, G. Garcia, ―Hybrid Control Law for a Three-Level NPC Rectifier‖, 18th European Control Conference (ECC), IEEE